

Research Paper

Sensitive detection of protein biomarkers using silver nanoparticles enhanced immunofluorescence assay

Li-Jun Zhao^{1*}, Ru-Jia Yu^{1*}, Wei Ma¹, Huan-Xing Han², He Tian¹, Ruo-Can Qian¹✉, Yi-Tao Long¹✉

1. Key Laboratory for Advanced Materials and Department of Chemistry, School of Chemistry and Molecular Engineering, East China University of Science and Technology, P. R. China.
2. Translational Medicine Center, Changzheng Hospital, the Second Military Medical University, P. R. China.

*These authors contributed equally.

✉ Corresponding authors: Y.T.L. (ytlong@ecust.edu.cn) or R.C.Q. (ruocanqianecust@163.com)

© Ivyspring International Publisher. This is an open access article distributed under the terms of the Creative Commons Attribution (CC BY-NC) license (<https://creativecommons.org/licenses/by-nc/4.0/>). See <http://ivyspring.com/terms> for full terms and conditions.

Received: 2016.09.14; Accepted: 2016.12.01; Published: 2017.02.08

Abstract

Detection of biomarkers is extremely important for the early diagnosis of diseases. Here, we developed an easy and highly sensitive fluorescence detection system for the determination of biomarkers by combining the rapid separation of magnetic beads and silver nanoparticles labeled antibodies. An ultrasensitive silver ions fluorescence probe 3', 6'-bis (diethylamino)-2-(2-iodoethyl) spiro[isoinidoline-1, 9'-xanthen]-3-one (Ag^+ -FP) was applied to immunoassay. A significant signal amplification was achieved as the AgNPs can be dissolved by H_2O_2 and generate numerous Ag^+ , which would turn "on" the fluorescence of Ag^+ -FP. Using α -fetoprotein (AFP) and C-reactive protein (CRP) as target analytes, good linear responses were obtained from 0.1 to 10 ng mL⁻¹ and the limits of detection (LOD) were as low as 70 pg mL⁻¹ and 30 pg mL⁻¹, respectively. In addition, the developed system was further evaluated for the detection of real samples including 30 positive serum specimens obtained from hepatocarcinoma patients and 20 negative serum samples, and performs as well as the commercial electrochemiluminescence immunoassay (ECLI) method with less cost and more convenience. Thus, the designed detection system can be used as a promising platform for the detection of a variety of biomarkers and served as a powerful tool in clinical diagnosis.

Key words: silver nanoparticles, magnetic beads, fluorescence detection, biomarkers.

Introduction

Currently, increasing attention has been paid to the development of robust, sensitive, and inexpensive detection methods to analyzing protein biomarkers, establishing a cornerstone of disease monitoring and diagnosis.[1, 2] Various advanced techniques, such as surface plasmon resonance[3], electrochemical[4, 5], quartz crystal microbalance[6] and optical analysis methods[7, 8] (including fluorescence and chemiluminescence) have been applied for the detection and quantification of biomarkers based on different respective signal generation principles.[9, 10] Among these approaches, fluorescence detection is the most widely applied approach due to its high sensitivity and easy combination with sandwich-type

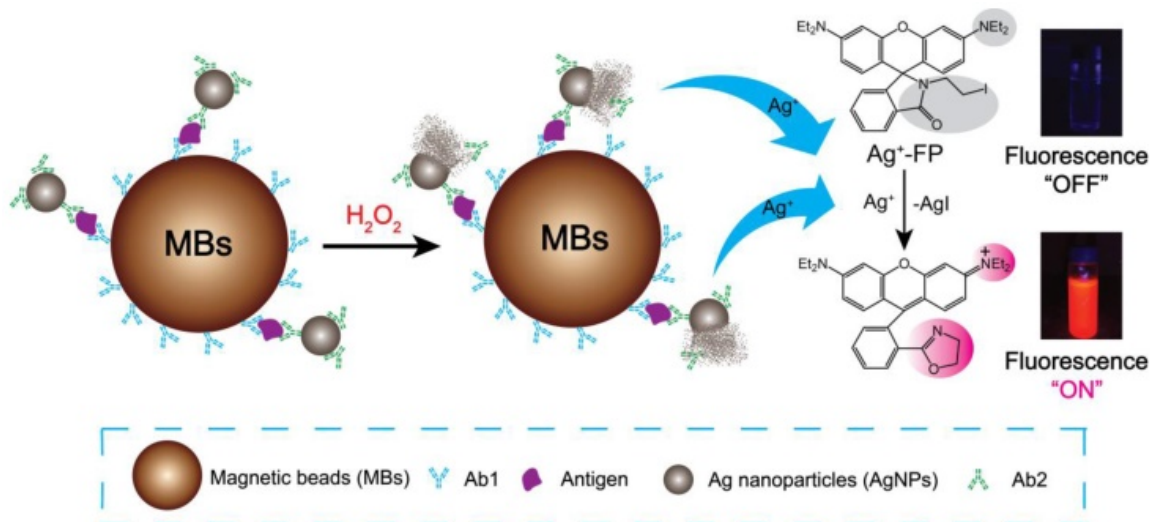
immuno-reactions.[11, 12] In spite of the successful development of fluorescence methods for the detection of various biomarkers, there are still some problems, such as limited signal amplification and unfavorable noise background.[13] Therefore, it is still a crucial challenge for the design of ultrasensitive strategies to improve the detection performance.

In the typical immunofluorescence assay methods, fluorescent labels (quantum dots, fluorescein) are mainly used as signal transduction materials by directly binding to antibodies for recognition with target analytes without amplification.[14] Therefore, the sensitivity of immunofluorescence assay is limited due to the

limited photostability of fluorescent labels and recognition abilities of antibodies.[15, 16] Several different strategies have been explored to solve the above problems, including the development of new fluorescent materials, the improvement of fluorescence detection instrument, the establishment of integrated analysis system.[17-21] Among these strategies, the application of functionalized nanomaterials has provided a new opportunity for the practical application of fluorescence techniques in biomarkers detection. Recent advancements in the fabrication of novel nanostructures have driven the fast development of various nanoparticles with special physical and chemical properties, such as high surface-to-volume ratio, unique optical, electronic, and biocompatible properties.[22] The high biocompatibility of these nanoparticles make them especially suitable for the application in bio-detection. Up to now, various nanoparticles including noble metal nanoparticles,[23] carbon nanomaterials,[24] metal oxide nanostructures,[25] and semiconductor nanocrystals[26] have been successfully used in fluorescence detection of various biomarkers. ZnO quantum dots have been used as direct fluorescent labels to detect carbohydrate antigen 19-9 (CA 19-9), which was a preferred marker for pancreatic cancer.[25] CuS NPs, which can oxidize non-fluorescent o-phenylenediamine to fluorescent 2, 3-diaminophenazine under physiological conditions, have been applied for the highly sensitive detection of prostate-specific antigen (PSA).[27] Gold nanoparticles, due to their strong fluorescent quenching activities have also been used to set up various fluorescence detection systems for the detection of human IgG and AFP antigen.[24, 25] Compared with these developed nanoparticles, silver

nanoparticles (AgNPs) are especially attractive due to their unique advantages, such as easy preparation of Ag hybridized composites,[28] catalyzed deposition,[29] and easy conversion to silver ions.[30] Fluorescence enhancement systems triggered by AgNPs have been reported,[31, 32] but have not been applied for immunofluorescence assay. In this case, we are inspired to design an improved fluorescence detection system for the sensitive detection of biomarkers using functionalized AgNPs.

Here, a novel fluorescence strategy based on AgNPs labeled antibodies was used for the detection of biomarkers. In our approach, each silver nanoparticle (AgNP) can be dissolved and produce millions of silver ions in the presence of hydrogen peroxide, which means the sensitivity of designed immunofluorescence assay method for the detection of biomarkers was seven magnitudes higher than Ag^+ -FP for the detection of Ag^+ . Magnetic beads (MBs) also was applied to the detection system due to its superior performances, such as high specific surface area, physical and chemical stability, low toxicity, good biocompatibility, and facile separation, purification, concentration processes. [33, 34] As shown in Scheme 1, for a certain type of biomarker, after the analytes were bound by Ab1-MBs, the Ab2-AgNPs were added into the mixture, and then the Ab2-AgNPs were captured on the surface of MBs through sandwich-type immuno-binding. The obtained sandwich-type immuno-complexes were collected via "one-step" magnetic separation, and the analyte-linked Ab2-AgNPs were dissolved in the mixed solution of Ag^+ -FP containing H_2O_2 . A significant signal amplification was achieved as the AgNPs dissolved by H_2O_2 and generated numerous Ag^+ , which turn "on" the fluorescence of Ag^+ -FP. The



Scheme 1. Schematic illustration of Ag^+ triggered fluorescence detection for protein biomarkers.

designed fluorescence detection system showed high sensitivity and excellent selectivity in the detection of biomarkers including α -fetoprotein (AFP), C-reactive protein (CRP) and human serum samples. Thus, a promising platform with low cost and ideal convenience has been achieved for the detection of biomarkers, providing a powerful tool in the clinical diagnosis.

Materials and Methods

Materials

The AFP antigen and antibodies, CRP antigen and antibodies, Carcino-embryonic antigen (CEA), prostate-specific antigen (PSA) and hepatitis B virus surface antigen (HBsAg) were provided by the Second Military Medical University, Shanghai, China. Amino-coated magnetic beads (MBs, particle size: ~ 500 nm) in an aqueous suspension with a concentration of 10 mg mL^{-1} were obtained from Beaver Nano-Technologies. Bovine serum albumin (BSA, 96 % – 99 %), trisodium citrate, and hydrogen peroxide were purchased from Sigma-Aldrich. Silver nanoparticles with different sizes (20, 40, 80 nm) in diameters were purchased from nanoComposix. All other reagents were of analytical grade and used without further purification. Ultrapure water obtained from a Millipore water purification system ($\geq 18 \text{ M}\Omega$, Milli-Q, Millipore) was used in all runs. The serum samples for AFP clinical diagnosis were provided by the Second Military Medical University, Shanghai. The binding and washing buffer solution (B&W) consisted of phosphate buffer saline PBS (20 mM, pH 7.4) with added 0.05 % (v/v) Tween 20 (pH 7.4). The measuring medium for the fluorescence measurements consisted of a 20 μM Rhodamine B-based Ag^+ fluorescence probe, 100 mM H_2O_2 , 1 μM H_3PO_4 and 20 % ethanol solution. For comparison, these specimens were assayed by the Second Military Medical University, Shang Hai, China using electrochemiluminescence immunoassay (ECLI) technique (Elecsys 2010, consisted of 20 mM phosphate-buffered saline).

A SpectraMax M5 plate reader (Molecular Devices, USA) was used for fluorescence measurement. UV-Vis spectra were obtained on an Ocean optical USB 2000+ UV-Vis spectrometer. Transmission electron microscopy (TEM) measurements were performed on a JEOL JEM-2010 with accelerating voltage 200 kV. Dark-Field Microscopy were obtained on an inverted microscope (eclipse Ti-U, Nikon, Japan) that was assembled with a dark-field condenser ($0.8 < \text{NA} < 0.95$) and a $40\times$ objective lens ($\text{NA} = 0.6$). The white light source was a 100 W halogen lamp. The AgNPs were immobilized on a platform, and the white light source

was used to excite the AgNPs to generate plasmon resonance scattering light. A true-color digital camera (Nikon DS-fi, Japan) was used to capture the dark-field color images.

Synthesis of Rhodamine B-based Ag^+ fluorescence probe ($\text{Ag}^+\text{-FP}$)

The Rhodamine B-based Ag^+ fluorescence probe 3', 6'-bis(diethylamino)-2-(2-iodoethyl)spiro [isoin-doline-1,9'-xa-nthen]-3-one ($\text{Ag}^+\text{-FP}$) was synthesized according to the published method and shown in Figure S1.[31] First, Rhodamine B reacted with 2-aminoethanol in ethanol at 120°C for 2 days obtained inter mediates 3', 6'-bis(diethylamino)-2-(2-hydroxyethyl)-3',9'-dihydrospiro[isoi-ndoline-1,9'-xanthen]-3-one (compound 1). The compound 1 was further allowed to react with methanesulfonyl chloride and sodium iodide to obtain the target compound ($\text{Ag}^+\text{-FP}$) by two steps reaction: methanesulfonyl reaction and iodide reaction. The structures of all compounds were characterized by ^1H NMR, ^{13}C NMR, HRMS spectra (supporting information).

Synthesis and characterization of 60 nm silver nanoparticles

The 60 nm diameter AgNPs were synthesized by the published method.[35, 36] Briefly, AgNO_3 (90 mg) was dissolved in 500 mL of H_2O and brought to boiling. Then a solution of 1 % sodium citrate (10 mL) was added and kept on boiling for 30 min. The size of AgNPs was characterized by UV-vis spectrum and TEM (Figure S2). The synthesized silver nanoparticles should be condensed by centrifugation and re-dispersed in phosphate buffer solution (1 mM, pH 7.4) for the following experiment.

The preparation of Ab2 conjugated AgNPs (Ab2-AgNPs)

The AgNPs with different sizes were used to the preparation of Ab2-AgNPs . Typically, 1 mL AgNPs were first mixed with 10 μL Ab2 solution (2 mg mL^{-1}). The mixture was shaken at 37°C for 12 h, and then 500 μL 1.0 wt % BSA solution was added and continued to shake at 37°C for 12 h. The solution was washed (2 times) with PBS (1 mM), centrifuged, and redispersed in 1 mL 0.1 wt % BSA. The resulting Ab2-AgNPs were stored at 4°C before use. The conjugation of labelled antibody Ab2 on the surface of silver nanoparticles AgNPs was evaluated by immunofluorescence experiments (Figure S3).

The preparation of magnetic beads immuno-complexes (Ab1-MBs@AG)

The amino-MBs (1 mL, 10 mg mL^{-1}) were first activated by reacting with 15 % fresh prepared

glutaraldehyde in PBS (20 mM, pH 7.4) for 12 h at 4 °C, and then washed thoroughly with deionized water to remove the excess glutaraldehyde (the reaction need to be performed in the dark condition to avoid glutaraldehyde polymerization). After magnetic separation, the glutaraldehyde-functionalized MBs (glu-MBs) were dispersed into 1 mL of PBS (50 mM, pH 7.4). Then 50 μ L of the glu-MB solution was added to 500 μ L of carbonate buffer (pH 9.6) containing 60 μ g of Ab1 and shaken overnight at 4 °C. Subsequently, 10 μ L of 5 wt % BSA in PBS (pH 7.2) was injected into the suspension and incubated for 2 h at 4 °C to block the possible residual sites on the MB. The conjugation of antibody Ab1 on the surface of MBs was evaluated by immunofluorescence experiments (Figure S4). Afterward, 100 μ L of antigen (AG) solution with different concentrations were added and incubated at 37 °C for 30 min to obtain the magnetic beads immuno-complex: Ab1-MBs@AG.

Detection protocol and spectrophotometric analysis

In a typical detection experiment, 50 μ L Ab1-MBs@AG solution was transferred into a 0.5-mL Eppendorf tube, and 100 μ L excess Ab2-AgNPs was added, the mixture was incubated for 30 min at 37 °C with gentle mixing in a TS-100 ThermoShaker to obtain the immuno-complexes Ab1-MBs@AG@Ab2-AgNPs. After magnetic separation, the Ab1-MBs@AG@Ab2-AgNPs were washed three times with 150 μ L of B&W buffer and transferred into each 96-well plates. Then, 100 μ L Ag⁺-FP solution comprised of 50 mM H₂O₂ and 20 % ethanolic water was added into each well, and reacted at room temperature for 30 min. The fluorescence intensity of each wells was then measured by SpectraMax M5 plate reader. The conjugation of Ab1-MBs@AG with Ab2-AgNPs was also characterized by TEM (Figure S5).

Results and Discussion

Principle and characteristics of the Ag⁺-triggered fluorescence detection system for biomarkers

In this work, the Ab1-MBs were prepared by direct immobilization of Ab1 on the surfaces of amino-MBs based on the aldehyde-ammonia condensation reactions. The amino-MBs were required to be simply activated by glutaraldehyde before binding with Ab1. Silver nanoparticles functionalized with corresponding Ab2 were utilized as labelled antibodies (Ab2-AgNPs). In a typical detection experiment, the target antigens were sandwiched between the Ab1-MBs and the

Ab2-AgNPs, generating immuno-complexes labelled Ab1-MBs@AG@Ab2-AgNPs. After the sandwich immuno-reaction, the Ag⁺-FP solution containing H₂O₂ was used to dissolve the AgNPs into numerous Ag⁺. For 60 nm AgNPs, a single AgNP can generate about ten millions Ag⁺, and each Ag⁺ can turn “on” the fluorescence of one Ag⁺-FP molecule. Thus, a significant signal amplification can be realized compared with the fluorescence detection of Ag⁺-FP for Ag⁺. By monitoring the variation of the fluorescence intensity, we can conveniently determine the concentration of target antigens with high sensitivity. Importantly, in the absence of the Ag⁺, the fluorescence of Ag⁺-FP probe was turned off, inducing an ultralow background noise, which was the key element for the establishment of our ultrasensitive fluorescence detection system.

Fluorescence response of Ag⁺-FP in the presence of Ag⁺

As described above, the amplification of the fluorescence signal was based on the formation of a large amount of silver ions dissolved from Ag NPs. Before the following detection experiments for biomarkers, the sensitivity of Ag⁺-FP to Ag⁺ was evaluated in priority. The detection limit of Ag⁺-FP toward Ag⁺ was investigated by plotting the fluorescence intensity (at 585 nm) versus the concentration of Ag⁺ (AgNO₃ was used as the silver ions source). As shown in Figure 1, the fluorescence intensity increased with the increase of Ag⁺ concentration, with a good linear relationship between the fluorescence intensity and the Ag⁺ concentrations (linear range: 0.2 μ M to 2 μ M). The LOD of Ag⁺-FP for Ag⁺ was determined to be as low as ~0.06 μ M (~6 ppb). In our system, the resource of Ag⁺ was 60 nm AgNPs, which can be dissolved in H₂O₂ to generate ten millions silver ions. Therefore, the LOD of probe Ag⁺-FP for target antigens can be calculated to be 0.06 pM.

Optimization of the Ag⁺-triggered fluorescence detection system for biomarkers determination

Ab2-AgNPs were prepared using AgNPs with different sizes (20, 40, 60 nm, and 80 nm), and their fluorescence response to AFP (10 ng mL⁻¹) were compared. As shown in Figure S4, the fluorescence intensity increased with the diameter of AgNPs from 20 to 60 nm. However, the signal intensity decreased as the diameter kept growing to 80 nm, which might be caused by the steric hindrance of particles with larger size. The immunoreaction was sterically inhibited by the large size or mass of the particle. Although larger AgNPs can generate more Ag⁺, larger

NPs are more likely to aggregate thus hindering the conjugation of antibodies to the surface.

In this case, 60 nm AgNPs were chosen to perform the following detection experiments for AFP and C-reactive protein (CRP). The variation of fluorescent intensity with different reaction time was investigated. (Figure S7). The fluorescence intensity increased with the longer incubation time, and reached a steady value after 2 h. From the above results, we chose 60 nm AgNPs and 2 h incubation time as the optimized conditions. The concentration of Ab2 used to modify AgNPs was optimized by AFP detection. As shown in Figure S8, the fluorescence response increased with the higher concentration of Ab2, and reached a maximum value at five times of Ab2 for AgNPs. Therefore, in the following experiment, a concentration of antibody at ten times for AgNPs was used for the modification.

Monitoring the dissolution process of AgNPs

The dissolution process of 60 nm AgNPs was observed by UV-Vis spectra and dark field imaging. As shown in Figure 2A, the absorption peak of AgNPs was observed at 420 nm. After the addition of H₂O₂, the absorption intensity decreased quickly and eventually disappeared within 5 min. In addition, dark-field microscope was also used to observe the dissolution process of AgNPs. As shown in Figure 2B, the green spots of AgNPs gradually disappeared after incubation with H₂O₂. These results indicated that the excellent dissolved ability of H₂O₂ for AgNPs.

Ag⁺-triggered fluorescence detection

Under optimal experimental conditions, the analytical performance of the Ag⁺-triggered fluorescence detection system was investigated by

detecting various concentrations of AFP. Figure 3A depicted the fluorescence emission spectra obtained from the fluorescence detection system in the presence of different human AFP concentrations. It was observed that the fluorescence intensity increased with the elevated AFP concentration over the range from 0 to 1000 ng mL⁻¹. The corresponding linear relationship between fluorescence intensity and the concentrations of AFP was obtained in the range from 0.1 ng mL⁻¹ to 10 ng mL⁻¹ (Figure 3B) with a linear correlation coefficient of 0.99, and the LOD was estimated to be ~70 pg mL⁻¹ (~1.0 pM). Compared with the other reported immunofluorescence methods for protein biomarkers, the designed method has a lower LOD (Table S1) and the sensitivity of the designed system is sufficient for the clinical applications.

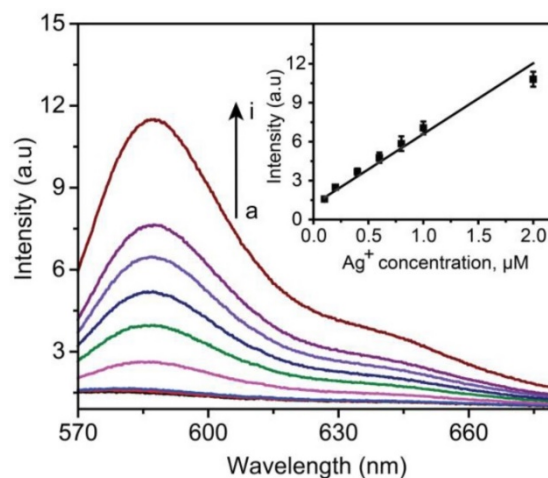


Figure 1. Fluorescence spectra of Ag⁺-FP (10 μM) in the presence of different concentrations of Ag⁺ (from a to i, 0, 0.001, 0.01, 0.2, 0.4, 0.6, 0.8, 1.0, 2.0 μM); inset: Calibration curves of fluorescence intensity versus the concentrations of Ag⁺ (ex: 530 nm; em: 585 nm), $Y = 5.446X + 1.146$, $R = 0.96$.

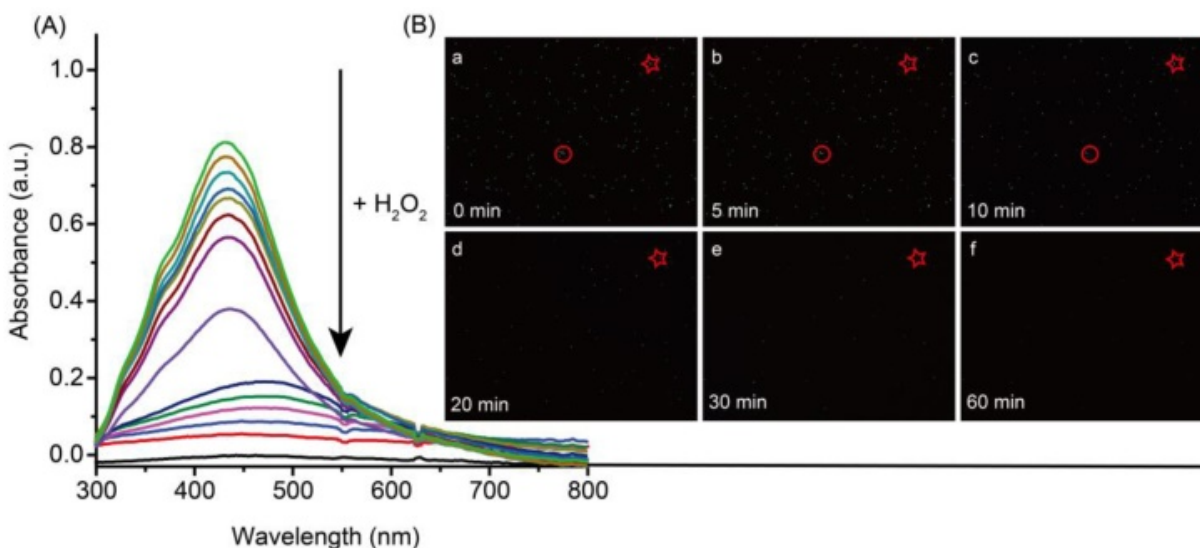


Figure 2. UV-Vis spectra (A) and dark-field images (B) of silver nanoparticles in the presence of 10 mM hydrogen peroxide. Dark-field imaging recorded the images of the AgNPs before (B-a) and after incubation with hydrogen peroxide for 5 min (B-b), 10 min (B-c), 15 min (B-d), 20 min (B-e) and 30 min (B-f).

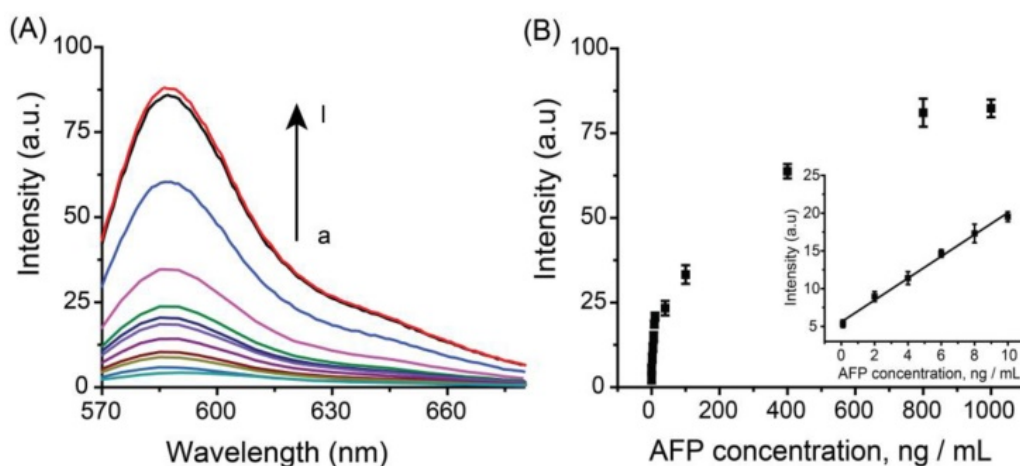


Figure 3. (A) Fluorescence spectra of the immuno-system with a series concentration of AFP (from a to I: 0, 0.1, 2, 4, 6, 8, 10, 40, 100, 400, 800, 1000 ng mL⁻¹, respectively). (B) Calibration curves of fluorescence intensity versus the concentrations of AFP. The inset indicates that the curve is linear over the range from 0.1 to 10 ng mL⁻¹, $Y = 1.449X + 5.566$, $R = 0.99$. The error bars represent the standard deviation of three measurements.

The specificity of the system to AFP was also evaluated using tumor markers carcinoembryonic antigen (CEA), C-reactive protein (CRP) and prostate-specific antigen (PSA), familiar pathogen hepatitis B virus surface antigen (HBsAg) and bovine serum (BSA). In this control experiment, 10 ng mL⁻¹ AFP was used as the target antigen, and a higher concentration (1.0 μg mL⁻¹) for other interferential proteins have been applied due to the complexities and uncertainties of real samples. As shown in Figure 4, negligible signals were observed using interfering proteins without cross-reactivity, showing high specificity of the system for AFP detection.

To verify the universality of the detection system, CRP, a pivotal biomarker for human inflammation and cardio-vascular diseases, was also performed using this system. A similar detection result was obtained. Figure 5A depicted the fluorescence emission spectra obtained from the fluorescence immunoassay system in response to different concentrations of human CRP. It was

observed that the fluorescence intensity increased with the rising of CRP concentration over the range from 0 to 1000 ng mL⁻¹. Meanwhile, a good linear relationship between the fluorescence intensity and the concentration of CRP in the range of 0.1 to 10 ng mL⁻¹ ($R = 0.9991$) (Figure 5B).

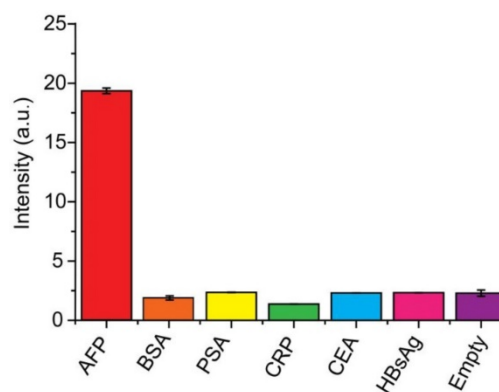


Figure 4. Specificity of the developed detection system for the determination of AFP. The concentration of AFP was 10 ng mL⁻¹ and the concentrations of other proteins (BSA, PSA, CRP, CEA and HBsAg) were 1.0 μg mL⁻¹.

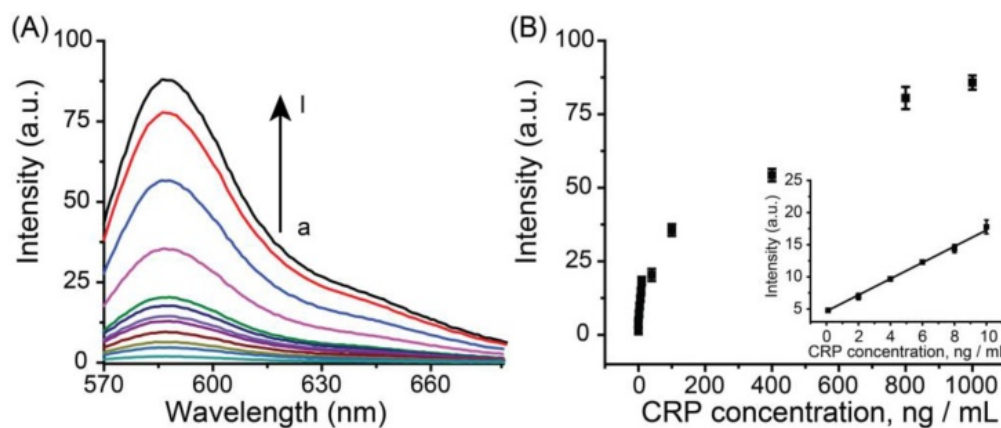


Figure 5. (A) Fluorescence spectra of the immuno-system with a series concentration of CRP (from a to I: 0, 0.1, 2, 4, 6, 8, 10, 40, 100, 400, 800, 1000 ng mL⁻¹, respectively). (B) Calibration curves of fluorescence intensity versus the concentrations of CRP. The inset indicates that the curve is linear over the range from 0.1 to 10 ng mL⁻¹, $Y = 1.261X + 4.656$, $R = 0.99$. The error bars represent the standard deviation of three measurements.

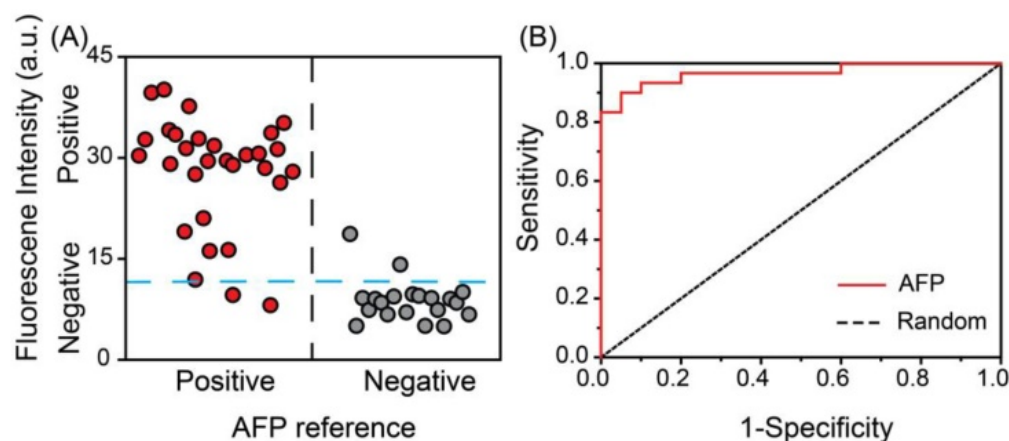


Figure 6. Double-blind experiment for the detection of AFP in serum samples from clinical patients. A) Vertical scatter plots of the values of fluorescence intensity for positive and negative samples (serum samples of AFP are represented by red solid circle for positive and gray solid circle for negative). B) Received-operating characteristic (ROC) curve.

The LOD was 30 pg mL^{-1} ($\sim 0.25 \text{ pM}$). The successful detection of CRP demonstrated good universality of this system.

Real sample detection of AFP. In order to test the practicality of the detection system in clinical diagnosis, a double-blind experiment was performed using 50 unrelated samples with a 10-fold dilution. As shown in Figure 6 the vertical scatter plots of the values of relative fluorescence intensity for positive and negative samples were made to estimate the accuracy of the proposed system (Figure 6A). The blue dotted line was marked as a threshold for positive and negative results of our assay. The red circles and gray circles represented for the positive and negative samples respectively, according to the data obtained from the ECLI method in hospital. It was observed that the diagnosis results using the developed fluorescence detection system were in good agreement with those determined by the commercial ECLI method, with the negative and positive percentage of agreement were 90.0 % (18/20) 93.3 % (28/30), respectively. The receiver operating characteristic (ROC) curve was also applied to survey the accuracy of the system (Figure 6B). The area under ROC curve (AUC) was calculated to be 0.96, indicating the high accuracy of this assay. Thus, the developed fluorescence detection system provides a feasible alternative method for determining AFP in human serum in clinical laboratory.

Conclusions

In conclusion, we have developed an easy Ag^+ -triggered fluorescence detection system for the determination of biomarkers, combining the advantages of rapid sample separation through MBs and highly efficient signal amplification using $\text{Ab}_2\text{-AgNPs}$. An ultrasensitive silver ions fluorescence probe, $\text{Ag}^+\text{-FP}$, was synthesized and used in the

immunoassay. This proposed fluorescence detection system showed good sensitivity and possibility for the detection of AFP and CRP, demonstrating an outstanding performance in clinical diagnosis of hepatocarcinoma patients. Therefore, the proposed system provided a promising universal platform for the detection of biomarkers for clinical diagnosis.

Supplementary Material

Supplementary figures and tables.

<http://www.thno.org/v07p0876s1.pdf>

Acknowledgements

This research was supported by the 973 Program (Grants 2013CB733700), the National Natural Science Foundation of China (No. 21327807, 21421004), and the Program of Shanghai Subject Chief Scientist (No. 15XD1501200), the Programme of Introducing Talents of Discipline to Universities (No. B16017).

Conflict of Interest

The authors declare no competing financial interest.

References

- Rittenour WR, Hamilton RG, Beezhold DH, Green BJ. Immunologic, spectrophotometric and nucleic acid based methods for the detection and quantification of airborne pollen. *J Immunol Methods*. 2012; 383:47-53.
- Qin Z, Chan WCW, Boulware DR, Akkin T, Butler EK, Bischof JC. Significantly Improved Analytical Sensitivity of Lateral Flow Immunoassays by Using Thermal Contrast. *Angew Chem Int Ed*. 2012; 124:4434-4437.
- Wasowicz M, Viswanathan S, Dvornyk A, Grzelak K, Kludkiewicz B, Radecka H. Biosens Bioelectron. 2008, 24, 191-197. Development of an oligo(ethylene glycol)-based SPR immunosensor for TNT detection. *Biosens Bioelectron*. 2008; 24:191-197.
- Lai G, Yan F, Wu J, Leng C, Ju HX. Ultrasensitive Multiplexed Immunoassay with Electrochemical Stripping Analysis of Silver Nanoparticles Catalytically Deposited by Gold Nanoparticles and Enzymatic Reaction. *Anal Chem*. 2011; 83:2726-2732.
- Deng XD, Chen MS, Fu Q, Smeets NMB, Xu F, Zhang ZY, Filipe CDM, Hoare T. A Highly Sensitive Immunosorbent Assay Based on Biotinylated Graphene Oxide and the Quartz Crystal Microbalance. *ACS Appl Mater Interfaces*. 2016; 8:1893-1902.
- Tang J, Zhou J, Li QF, Tang DP, Chen GN, Yang HH. In situ amplified electronic signal for determination of low-abundance proteins coupling with nanocatalyst-based redox cycling. *Chem Commun*. 2013; 49:1530-1532.

7. Yang QQ, Zhu JG, Ma F, Li PW, Zhang LX, Zhang W, Ding XX, Zhang Q. Quantitative determination of major capsaicinoids in serum by ELISA and time-resolved fluorescent immunoassay based on monoclonal antibodies. *Biosens Bioelectron.* 2016; 81:229-235.
8. Yang Z, Fu Z, Yan F, Liu H, Ju H. A chemiluminescent immunosensor based on antibody immobilized carboxylic resin beads coupled with micro-bubble accelerated immunoreaction for fast flow-injection immunoassay. *Biosens Bioelectron.* 2008; 24:35-40.
9. Tang D, Niessner R, Knopp D. Flow-injection electrochemical immunosensor for the detection of human IgG based on glucose oxidase-derived biomimetic interface. *Biosens Bioelectron.* 2009; 24:2125-2130.
10. Tang D, Yuan R, Chai Y. Ultrasensitive Electrochemical Immunosensor for Clinical Immunoassay Using Thionine-Doped Magnetic Gold Nanospheres as Labels and Horseradish Peroxidase as Enhancer. *Anal Chem.* 2008; 80:1582-1588.
11. Giljohann DA, Mirkin CA. Drivers of biodiagnostic development. *Nature* 2009; 462:461-464.
12. Pei X, Zhang B, Tang J, Liu B, Lai W, Tang D. Sandwich-type immunosensors and immunoassays exploiting nanostructure labels: A review. *Anal Chim Acta.* 2013; 758:1-18.
13. Tang D, Yu Y, Niessner R, Miro M, Knopp D. Magnetic bead-based fluorescence immunoassay for aflatoxin B1 in food using biofunctionalized rhodamine B-doped silica nanoparticles. *Analyst.* 2010; 135:2661-2667.
14. Wang H, Kim Y, Liu H, Zhu Z, Bamrungsap S, Tan W. Engineering a unimolecular DNA-catalytic probe for single lead ion monitoring. *J Am Chem Soc.* 2009; 131:8221-8226.
15. Chen Y, Munteanu AC, Huang YF, Phillips J, Zhu Z, Mavros M, Tan W. Mapping receptor density on live cells by using fluorescence correlation spectroscopy. *Chem Eur J.* 2009; 15:5327-5336.
16. Wang L, Wang K, Santra S, Zhao X, Hilliard LR, Smith JE, Wu Y, Tan W. Watching silica nanoparticles glow in the biological world. *Anal Chem.* 2006; 78:646-654.
17. Huang Fu ZZ, Hao LJ, Wu YM, Qiao HY, Yi Z, Li XY, Chu X. Highly sensitive fluorescent immunoassay of human immunoglobulin G based on PbS nanoparticles and DNAzyme. *Anal Sci.* 2013; 29:499-504.
18. Si Z, Li Y, Quan H, Qi H, Li T, Yang M. ELISA type fluorescence turn-on immunoassay based on Fe³⁺ induced fluorescence enhancement. *Sens Actuators B: Chem.* 2014; 202:663-666.
19. Yan J, Estévez MC, Smith JE, Wang K, He X, Wang L, Tan W. Dye-doped nanoparticles for bioanalysis. *Nano Today* 2007; 2:44-50.
20. Huhtinen P, Kivelä M, Kuronen O, Hagren V, Takalo H, Tenhu H, Lövgren T, Härmä H. Synthesis, Characterization, and Application of Eu(III), Tb(III), Sm(III), and Dy(III) Lanthanide Chelate Nanoparticle Labels. *Anal Chem.* 2005; 77:2643-2648.
21. Wang L, Yang C, Tan W. Dual-Luminophore-Doped Silica Nanoparticles for Multiplexed Signaling. *Nano Lett.* 2005; 5:37-43.
22. Della Pina C, Falletta E, Prati L, Rossi M. Selective oxidation using gold. *Chem Soc Rev.* 2008; 37:2077-2095.
23. Ambrosi A, Castañeda MT, Killard AJ, Smyth MR, Alegret S, Merkoçi A. Double-Codified Gold Nanolabels for Enhanced Immunoanalysis. *Anal Chem.* 2007; 79:5232-5240.
24. So HM, Won K, Kim YH, Kim BK, Ryu BH, Na P-S, Kim H, Lee JO. Single-Walled Carbon Nanotube Biosensors Using Aptamers as Molecular Recognition Elements. *J Am Chem Soc.* 2005; 127:11906-11907.
25. Gu B, Xu C, Yang C, Liu S, Wang M. ZnO quantum dot labeled immunosensor for carbohydrate antigen 19-9. *Biosens Bioelectron.* 2011; 26:2720-2723.
26. Sheng Z, Han H, Hu D, Liang J, He Q, Jin M, Zhou R, Chen H. Quantum dots-gold(III)-based indirect fluorescence immunoassay for high-throughput screening of APP. *Chem Commun.* 2009; 18:2559-2561.
27. Zhu YD, Peng J, Jiang LP, Zhu JJ. Fluorescent immunosensor based on CuS nanoparticles for sensitive detection of cancer biomarker. *Analyst.* 2014; 139:649-655.
28. Su B, Tang D, Li Q, Tang J, Chen G. Gold-silver-graphene hybrid nanosheets-based sensors for sensitive amperometric immunoassay of alpha-fetoprotein using nanogold-enclosed titania nanoparticles as labels. *Anal Chim Acta.* 2011; 692:116-124.
29. Lai G, Yan F, Wu J, Leng C, Ju H. Ultrasensitive Multiplexed Immunoassay with Electrochemical Stripping Analysis of Silver Nanoparticles Catalytically Deposited by Gold Nanoparticles and Enzymatic Reaction. *Anal Chem.* 2011; 83:2726-2732.
30. Tung NH, Chikae M, Ukita Y, Viet PH, Takamura Y. Sensing Technique of Silver Nanoparticles as Labels for Immunoassay Using Liquid Electrode Plasma Atomic Emission Spectrometry. *Anal Chem.* 2012; 84:1210-1213.
31. Chatterjee A, Santra M, Won N, Kim S, Kim JK, Kim SB, Ahn KH. Selective fluorogenic and chromogenic probe for detection of silver ions and silver nanoparticles in aqueous media. *J Am Chem Soc.* 2009; 131:2040-2041.
32. Suslov A, Lama PT, Dorsinville R. Fluorescence enhancement of Rhodamine B by monodispersed silver nanoparticles. *Opt Commun.* 2015; 435:116-119.
33. Pedrero M, Campuzano S, Pingarron JM. Magnetic beads-based electrochemical sensors applied to the detection and quantification of bioterrorism/biohazard agents. *Electroanal.* 2012; 24:470-482.
34. Ding Y-D, Cong T, Chu XY, Jia Y, Hong X, Liu YC. Magnetic-bead-based sub-femtomolar immunoassay using resonant Raman scattering signals of ZnS nanoparticles. *Anal Bioanal Chem.* 2016; 408:5013-5019.
35. Wan Y, Guo Z, Jiang X, Fang K, Lu X, Zhang Y, Gu N. Quasi-spherical silver nanoparticles: Aqueous synthesis and size control by the seed-mediated Lee-Meisel method. *J Colloid Interface Sci.* 2013; 394:263-268.
36. Tang L, Li S, Han F, Liu L, Xu L, Ma W, Kuang H, Li A, Wang L, Xu C. SERS-active Au@Ag nanorod dimers for ultrasensitive dopamine detection. *Biosens Bioelectron.* 2015; 71:7-12.